

## NOTES AND CORRESPONDENCE

## On the Numerical Simulation of Graupel/Hail Initiation via the Riming of Snow in Bulk Water Microphysical Cloud Models

RICHARD D. FARLEY, PAMELA E. PRICE, HAROLD D. ORVILLE AND JOHN H. HIRSCH

*Institute of Atmospheric Sciences, South Dakota School of Mines and Technology, Rapid City, South Dakota*

5 May 1988 and 30 September 1988

## 1. Introduction

The purpose of this note is to illustrate a theoretical and practical modification to the modeling of snow and graupel/hail formation in cloud models using "bulk water" cloud microphysical processes based on Lin et al. (1983). This microphysical framework has been used by several investigators (Rutledge and Hobbs 1983; Lord et al. 1984; Krueger et al. 1986; Lesins and Lin 1986; Proctor 1987). As formulated in Lin et al., snow began to form graupel via an aggregation process after the snow mixing ratio passed a certain threshold (primarily via the accretion of supercooled cloud water). The modification described within this note allows the above process plus the formation of graupel/hail via snow (of a certain critical size) accreting supercooled cloud water as explained below. The formulation developed to simulate the riming of snow to form graupel/hail is based rather loosely on the work of Heymsfield (1982). It is an appropriate topic for the "Gagin Memorial Volume" because of Abe Gagin's interest in the precipitation problem and his excellent observations of the importance of graupel formation to precipitation in the Israeli clouds (Gagin 1981).

## 2. Snow production

First, the production term for snow at temperatures below 0°C is written symbolically as

$$P_S = P_{SAUT} + P_{SACI} + P_{SACW}(\delta_5) + P_{SFW} + P_{SFI} \\ + P_{RACI}(\delta_3) + P_{IACR}(\delta_3) - P_{GACS} - P_{GAUT} \\ - P_{WACS}(1 - \delta_4) - P_{RACS}(1 - \delta_2) \\ + P_{SACR}(\delta_2) + P_{SSUB}(1 - \delta_1) + P_{SDEP}(\delta_1), \quad (1)$$

where  $\delta_1$  through  $\delta_5$  are defined as

$$\delta_1 = \begin{cases} 1, & \text{for } l_{CW} + l_{CI} > 0 \\ 0, & \text{otherwise} \end{cases}$$

$$\delta_2 = \begin{cases} 1, & \text{for } l_R \text{ and } l_S < 10^{-1} \text{ g kg}^{-1} \\ 0, & \text{otherwise} \end{cases}$$

$$\delta_3 = \begin{cases} 1, & \text{for } l_R < 10^{-1} \text{ g kg}^{-1} \\ 0, & \text{otherwise} \end{cases}$$

$$\delta_4 = \begin{cases} 1, & \text{for } l_S < 10^{-1} \text{ g kg}^{-1} \text{ or } l_{CW} < 1 \text{ g kg}^{-1} \\ 0, & \text{otherwise} \end{cases}$$

$$\delta_5 = \begin{cases} 1, & \text{for } l_S < 10^{-1} \text{ g kg}^{-1} \text{ or } l_{CW} < 1 \text{ g kg}^{-1} \\ \gamma, & \text{otherwise,} \end{cases}$$

where  $\gamma = P_{SACWS}/P_{SACW}$  (as defined below). The symbols  $l_{CW}$ ,  $l_{CI}$ ,  $l_R$ , and  $l_S$  represent the cloud water, cloud ice, rain, and snow mixing ratios, respectively.

Most of the terms in (1) are derived in Lin et al. (1983), and this note will employ the same set of symbols and conventions. The symbols stand for snow autoconversion (aggregation -  $P_{SAUT}$ ), snow accreting cloud ice ( $P_{SACI}$ ), snow accreting cloud water ( $P_{SACW}$ ), snow formed via the Bergeron process ( $P_{SFW}$  and  $P_{SFI}$ ), the rate of snow (or graupel) formation by the interaction of rain and cloud ice ( $P_{RACI}$  and  $P_{IACR}$ ), graupel accreting snow ( $P_{GACS}$ ), snow aggregation to form graupel ( $P_{GAUT}$ ), the rate of snow conversion to graupel via the riming of the snow ( $P_{WACS}$ ), the rate of snow (or graupel) formation by the interaction of snow and rain ( $P_{RACS}$  and  $P_{SACR}$ ) and sublimation or deposition of water vapor on snow ( $P_{SSUB}/P_{SDEP}$ ).

Only the two terms affected by  $\delta_5$  and  $\delta_4$  are involved in the riming of snow to form graupel. These are explained in greater detail in the remainder of this note.

Originally,  $P_{SACW}$  represented a *two-component* freezing process. As defined in Lin et al. (1983), this is one in which the interaction between the liquid (cloud water) and solid (snow) particles leads to an increase in the mass of the solid particles (snow) and a decrease in cloud water. With the addition of the riming mechanism, the interaction between liquid and solid particles can result in *new* solid particles (graupel/hail). This becomes now a *three-component* freezing process, similar to the interaction of rain and cloud ice ( $P_{RACI}/P_{IACR}$ ), which results in either snow or hail (Lin et al. 1983); see Fig. 1a.

Corresponding author address: Richard D. Farley, Institute of Atmospheric Sciences, South Dakota School of Mines & Technology, Rapid City, SD 57701.

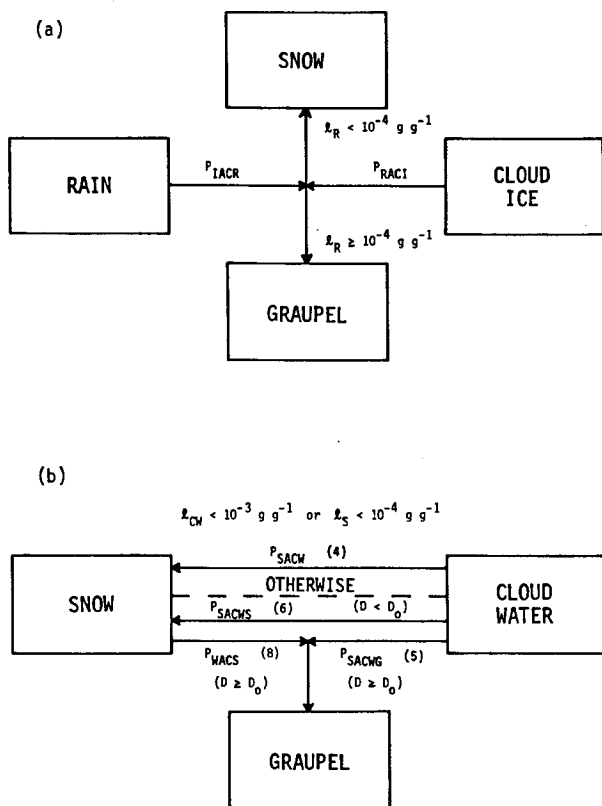


FIG. 1. (a) A flow chart of the normal three-component microphysical process. (b) A combined three-component and two-component process. The symbols are explained in the text.

However, the snow/cloud water interaction is unique in the model in that all other freezing processes are either two or three-component at any given grid point. The riming process for snow will be both two and three-component when the required thresholds are exceeded; the snow particles greater than some specified diameter,  $D_0$ , will rim into graupel/hail (three-component), while those smaller continue to grow by riming as they did in the original  $P_{SACW}$  process (two-component).

From Chang (1977) and Lin et al. (1983),  $P_{SACW}$  is the growth rate of snow particles based on geometric sweepout and subsequent freezing of cloud water droplets, with the growth of a single snow particle given by

$$\left. \frac{dM_s}{dt} \right|_{ACW} = E_{SW} \rho l_{CW} U_{DS} \pi D_s^2 / 4, \quad (2)$$

where  $E_{SW}$  is the collection efficiency of the snow for cloud water and is assumed equal to one. The terminal velocity of a snowflake of diameter  $D_s$  is represented by  $U_{DS}$ , and  $\rho$  is the density of air. Multiplying by  $N_{DS}$ , the number concentration of snow particles of size  $D_s$  and integrating (2) over the range of snowflake diameters from zero to infinity results in the total rate

of change of snow due to accretion of cloud water. This may be written as

$$P_{SACW} = \int_0^\infty E_{SW} l_{CW} U_{DS} N_{DS} (\pi D_s^2 / 4) dD_s. \quad (3)$$

Substituting appropriate relationships into (3) and performing the integration results in the following expression for snow accreting cloud water as given by Lin et al. (1983)

$$P_{SACW} = E_{SW} \pi n_{0S} c l_{CW} \Gamma(3 + d) (\rho_0 / \rho)^{1/2} / 4 \lambda_S^{3+d}. \quad (4)$$

In (4),  $n_{0S}$  and  $\lambda_S$  are the intercept and slope parameters for the assumed snow size distribution,  $c$  and  $d$  are the coefficient and exponent of the power law defining the terminal velocity of snow, and  $\rho_0$  is the air density at the surface. For a two-component process,  $P_{SACW}$  is a sink for cloud water and a source for snow. For the new three-component process, the integral in (3) is split into two parts, one integral from zero to  $D_0$ , and the second from  $D_0$  to infinity. However, this split results in two equations with closed form solutions which require the calculation of appropriate incomplete gamma functions. Since the calculation of incomplete gamma functions is computationally expensive, the solutions are found numerically instead, using Simpson's one-third rule to approximate the integral from  $D_0$  to infinity. For graupel production, (4) becomes

$$P_{SACWG} = \frac{1}{4} E_{SW} l_{CW} n_{0S} \left( \frac{\rho_0}{\rho} \right)^{1/2} \pi c \times \sum_{D_0}^{D_\infty} D_s^{d+2} \exp(-\lambda_S D_s) \Delta D_s, \quad (5)$$

which is a source for graupel and a sink for cloud water. Then

$$P_{SACWS} = P_{SACW} - P_{SACWG}, \quad (6)$$

which is a source for snow and a sink for cloud water (see Fig. 1b). In the above,  $\Delta D_s = 0.05$  cm and  $D_\infty$  is set at 2 cm, beyond which the mass of snow existing is negligible ( $<0.006\%$  for  $l_S = 4$  g  $kg^{-1}$ ) for the as-

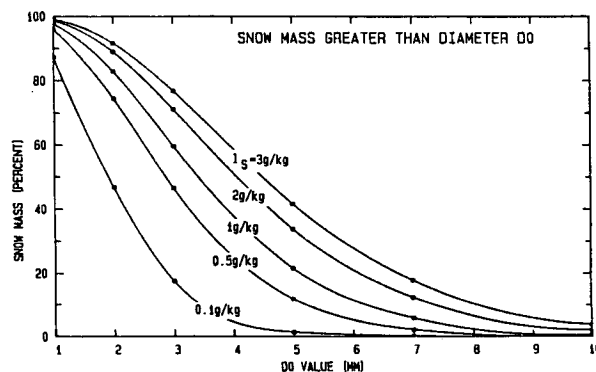


FIG. 2. The percentage of the snow mass that has a diameter greater than  $D_0$  for several different snow mixing ratios, ( $l_S$ ).

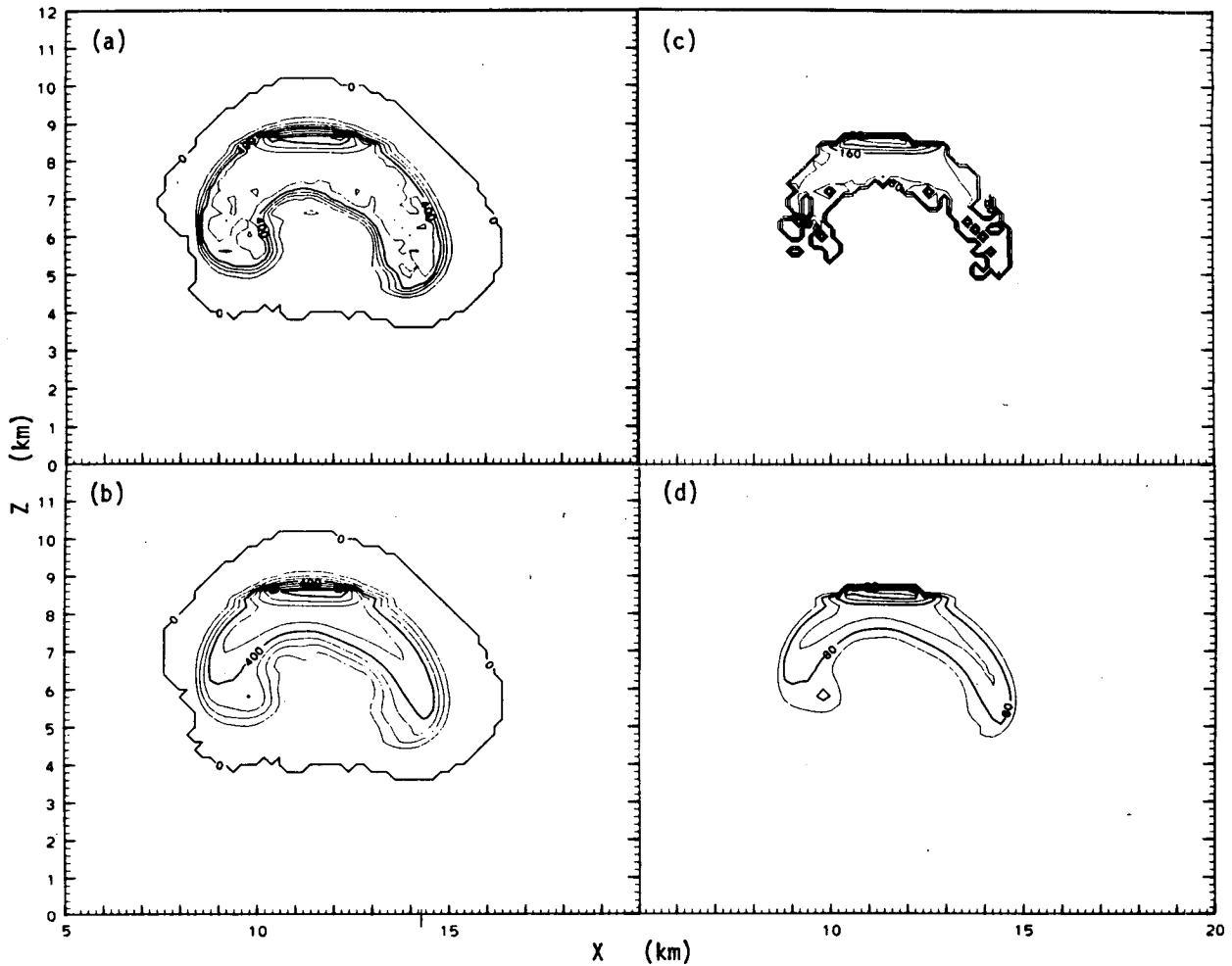


FIG. 3. Comparison of the snow field and the rate of snow conversion to graupel/hail ( $P_{WACS}$ ) for different values of the snow riming threshold. All panels are from a natural case simulation at 21 min. Panels (a) and (b) show the snow field, and panels (c) and (d) show the corresponding hail production rates for snow riming thresholds of 0.5 and 0.05  $\text{g kg}^{-1}$ , respectively. The maximum value of the hail production is  $3.3 \times 10^{-5} \text{ g g}^{-1} \text{ s}^{-1}$  in (c), and  $3.5 \times 10^{-5} \text{ g g}^{-1} \text{ s}^{-1}$  in (d). The value of  $D_0$  is 0.5 cm in both cases.

sumed exponential size distribution. The error involved in using the summation in (5) instead of the incomplete gamma function is less than 0.1% (for  $D_0 = 0.7$  cm), and the computation time is reduced by over an order of magnitude.

The amount of snow rimed into graupel for this three-component process is represented by  $P_{WACS}$ . It is equal to the mass of snow particles with diameters greater than  $D_0$  per unit mass of air divided by the time step (for consistent units). This converts the percentage of snow mass greater than  $D_0$  to graupel/hail at each time step. Figure 2 gives the percentage of snow mass greater than  $D_0$  for several different snow mixing ratios. For  $D_0$  equal to 0.7 cm, which is the value assumed in applications of the scheme, 18% of the snow mass is converted to graupel per time step when the snow content is  $3 \text{ g kg}^{-1}$ , while only 2% is converted for a snow content of  $0.5 \text{ g kg}^{-1}$ .

The derivation of  $P_{WACS}$  begins with the definition of  $l_s$  (in  $\text{g g}^{-1}$ ), which may be written as

$$l_s = n_{0S} \frac{\pi \rho_S}{6 \rho} \int_0^\infty D_S^3 \exp(-\lambda_S D_S) dD_S, \quad (7)$$

where  $\rho_S$  is the density of snow. The  $P_{WACS}$  is found by integrating (7) from  $D_0$  to infinity and dividing by the time step (3.75 s). The result is

$$P_{WACS} = \frac{n_{0S} \pi \rho_S}{6 \rho \lambda_S \Delta t} \exp(-\lambda_S D_0) \times \left[ D_0^3 + \frac{3D_0^2}{\lambda_S} + \frac{6D_0}{\lambda_S^2} + \frac{6}{\lambda_S^3} \right]. \quad (8)$$

Equations (5), (6), and (8) are used if both the snow and cloud water meet their mass thresholds of 0.1 and  $1.0 \text{ g kg}^{-1}$ , respectively. If not, (4) is used as a snow source, see Fig. 1b. For the density levels over which it is applied, the  $1.0 \text{ g kg}^{-1}$  threshold for cloud water is roughly equivalent to the lower limit of  $0.5 \text{ g m}^{-3}$  suggested by Heymsfield (1982). The snow threshold was initially tested at  $0.5 \text{ g kg}^{-1}$ , but this caused abnormal discontinuities to develop in the snow field

which amplified with time and the snow field became very unsmooth at its lower boundary. A threshold of  $0.05 \text{ g kg}^{-1}$  results in a much smoother field with only minor changes to the cloud water field. Although the change results in earlier snow riming, the snow mass is smaller at that time, and the amount converted is smaller. The overall effect of using the lower threshold is slightly faster but more continuous riming conversion from snow to hail. Figures 3a and 3b show the improvement in the snow field at 21 min when the threshold is lowered from 0.5 to  $0.05 \text{ g kg}^{-1}$ . Figures 3c and 3d, which are examples of output from a special microphysical analysis program, show the rates at which snow is converted to hail through riming ( $P_{\text{WACS}}$ ). In both cases, the maxima are located at upper levels, but the lower area of Fig. 3c is very ragged and affects the snow field similarly. This effect occurs for several minutes of simulated time. At later times, the  $0.5 \text{ g kg}^{-1}$  threshold run has so little snow left that the term is only in effect at certain points and is very unsmooth. The complimentary field,  $P_{\text{SACWG}}$ , shows a similar structure but at reduced rates, generally lower by a factor of 20 or more. Following these initial tests, the snow threshold was set to  $0.1 \text{ g kg}^{-1}$  to be more consistent with the other model thresholds. This value maintains the improved structure of the fields noted for the  $0.05 \text{ g kg}^{-1}$  threshold and results in a slight delay in the onset of the process.

Price (1985) and Price et al. (1986) report on a series of six simulations as an initial evaluation of this riming formulation. This involved natural, dry ice seeded, and silver iodide seeded cases with and without the riming formulation actively applied to a strong convective case from the North Dakota Weather Modification Project. The addition of the riming process causes significant changes in the model simulations, especially in the natural case. The natural snow field, which grows very large due to accretion of cloud water in the case without riming, is decreased by riming as the rimed snow is converted to graupel. With riming included, the differences between the seeded and nonseeded cases are reduced. The natural hail field develops slightly earlier at the expense of the snow and reaches an earlier peak, with timing similar to that of the seeded cases. The riming process has a strong impact for a limited time period following snow initiation, while the snow and cloud water coexist within the developing cloud. At later times, the snow exists mostly in the upper levels of the cloud, while the cloud water exists in the lower portions of the cloud and the interaction between the two fields is reduced. The spatial tendencies and reduced maximum values of the snow field are consistent with the results of a similar model which treats the precipitating ice field in greater detail using a discrete number of size categories (Farley 1987). For a more detailed discussion of these model comparisons, the reader is referred to the extended summary in Price et al. (1986) or the more extensive discussions in Price (1985), which is available upon request.

Further tests on smaller clouds are needed. The HI-PLEX test clouds would appear to be excellent candidates, as well as the 19 July 1981 CCOPE case, which has been simulated successfully (Helsdon and Farley 1987; Banta and Hanson 1987) and has been used as a test case in cloud modeling workshops.

*Acknowledgments.* We thank Mrs. Joie Robinson for typing the text and arranging the illustrations. The work was supported by the North Dakota Atmospheric Resource Board under Contract ARB-IAS-87-1 and the National Science Foundation under Grant ATM-8516940. Most of the computations were performed using the facilities of the Scientific Computing Division of the National Center for Atmospheric Research, which is sponsored by the National Science Foundation.

#### REFERENCES

- Banta, R., and K. R. Hanson, 1987: Sensitivity studies on the continentality of a numerically simulated cumulonimbus. *J. Climate Appl. Meteor.*, **26**, 275–286.
- Chang, C-H., 1977: Ice generation in clouds. M.S. thesis, Dept. of Meteorology, South Dakota School of Mines and Technology, Rapid City, 129 pp.
- Farley, R. D., 1987: Numerical modeling of hailstorms and hailstone growth: Part III. Simulation of an Alberta hailstorm—natural and seeded cases. *J. Climate Appl. Meteor.*, **26**, 789–812.
- Gagin, A., 1981: The Israeli rainfall enhancement experiment—a physical overview. *J. Wea. Modif.*, **13**, 108–120.
- Helsdon, J. H. Jr., and R. D. Farley, 1987: A numerical modeling study of a Montana thunderstorm: Part I: Model results versus observations involving non-electrical aspects. *J. Geophys. Res.*, **92**, 5645–5659.
- Heymsfield, A. J., 1982: A comparative study of the rates of development of potential graupel and hail embryos in High Plains storms. *J. Atmos. Sci.*, **39**, 2867–2897.
- Krueger, S., R. K. Wakimoto and S. J. Lord, 1986: Role of ice-phase microphysics in dry microburst simulations. *Joint Sessions 23rd Conf. Radar Meteorology and Conf. Cloud Physics, Vol. 3*, J73–76.
- Lesins, G., and Y. Lin, 1986: Precipitation efficiency calculations from a bulk microphysical kinematic cloud model. *Joint Sessions 23rd Conf. Radar Meteorology and Conf. Cloud Physics, Vol. 3*, J46–J48.
- Lin, Y-L., R. D. Farley and H. D. Orville, 1983: Bulk parameterization of the snow field in a cloud model. *J. Climate Appl. Meteor.*, **22**, 1065–1092.
- Lord, S. J., H. E. Willoughby and J. M. Piotrowicz, 1984: Role of a parameterized ice phase microphysics in an axisymmetric, non-hydrostatic tropical cyclone model. *J. Atmos. Sci.*, **41**, 2836–2848.
- Price, P. E., 1985: Microphysical model comparisons of seeded and non-seeded North Dakota clouds. M.S. thesis, Dept. of Meteorology, South Dakota School of Mines and Technology, Rapid City, 70 pp.
- , R. D. Farley, J. H. Hirsch and H. D. Orville, 1986: Microphysical model comparisons of seeded and non-seeded North Dakota clouds. *Preprints Tenth Conf. Weather Modification*, Arlington, Amer. Meteor. Soc., 159–164.
- Proctor, F. H., 1987: The terminal area simulation system. Vol. I: Theoretical formulation. NASA Rep. No. CR-4046, 123 pp.
- Rutledge, S. A., and P. V. Hobbs, 1983: The mesoscale and microscale structure and organization of clouds and precipitation in mid-latitude cyclones. VIII: A model for the “seeder-feeder” process in warm frontal rainbands. *J. Atmos. Sci.*, **40**, 1185–1206.